Differentially Fed Dual Band Directional Monopole Antenna Array for Wireless Communication

Md Nazmul Hasan
School of Electrical and Computer Engineering
Sungkyunkwan University
Suwon, South Korea
mnazmulh@ieee.org

Son Chu
Department of Engineering Science
University of Oxford
Oxford, UK
son.chu@eng.ox.ac.uk

Atiq Ben Ahmed
Tensorbundle Lab
Seoul, South Korea
abahmed@ieee.org

Nguyen Canh Minh
School of Electrical and Electronics Engineering
University of Transport and Communications
Hanoi, Vietnam
ncminh@utc.edu.vn

Can C. Chu
School of Electrical and Electronics Engineering
University of Transport and Communications
Hanoi, Vietnam
chucongcan@utc.edu.vn

***Abstract*—A dual band 2×2 monopole antenna array is proposed. The antenna array elements are fed differentially to align the radiated electric fields so that vectorial addition can be maximized to yield a high gain. Differential feeding is implemented by a 180-degree phase inverter placed in the feeding network. To avoid backside radiation, a metal reflector is placed beneath the ground plane. The proposed antenna operates at 2.75 GHz and 4.7 GHz, yielding a peak gain of 10 dBi and 6.51 dBi respectively. The proposed antenna array exhibits a broadside radiation patterns at the operating frequencies.**

***Index Terms*—monopole antenna, high gain, antenna array, phase inverter, planar antenna.**

I. Introduction

Printed antennas have become extremely popular for their compact size, and ease of integration with rest of the system blocks in portable devices [1]–[3]. Among the printed antennas that exploit standard printed circuit board fabrication technology, monopole antenas are widely used for their wide impedance bandwith and omnidirectional radiation pattern [4]–[6]. In some specific wireless communication applications, dual band planar antennas are essential. Operation at two different frequencies by employing only a single antenna can save system overhead significantly. A meandered monopole is reported to achieve dual band operation at 2.4 GHz and 5 GHz by introducing a protruded tuning stub into the meandered monopole structure [7]. Another folded monopole antenna with a defected ground structure (DGS) is reported to obtain dual resonance at 2.4 GHz and 5 GHz [8]. Tunable dual band planar antenna consisting of two patches suspended above a ground plane is reported in [9]. Combining the zeroth order resonant mode and TM_{02} mode, another monopolar patch antenna is reported to achieve dual band operation [10]. By combining a U-shaped electric dipole with a folded shorted patch assembled vertically on the ground plane, a dual band antenna is proposed in [11]. A U-slot is cut into the rectangular patch to obtain dual band resonance in [12].

Gain enhancement of planar antennas has been reported in several previous works by employing shorting pins [13], artifical magnetic conductor (AMC) structure [14], H-shaped resonator [15] and integrated phase inverter with back-side reflector [16], [17].

In this work, a dual band directional monopole antenna array is proposed. High gain is obtained by aligning the radiated electric fields of the array elements with the aid of a 180 degree phase inverter and a metal reflector that enhances the broadside radiation at the top. The proposed antenna array is designed and simulated in the commercial full-wave electromagnetic solver ANSYS HFSS.

The rest of the paper is organized as follows. In section II, the antenna array structure is described. Then, section III presents the simulation results of the antenna performance. Finally, concluding remarks are drawn in section IV.

II. Proposed Antenna Design

A. Antenna Geometry

The proposed 2×2 antenna array consists of four identical monopole elements of length s, see Fig. 1a. The array elements are fed by microstrip lines and T-junctions. The feeding network contains a tapered microtsrip line T-junction which excites the left and right 1×2 monopole sub-arrays. In one of the T-junction arms, there lies a 180 degree phase inverter as shown in Fig. 1a. The details design of the phase inverter is described in the next subsection. Fig. 1b shows the ground plane of the antenna. The ground plane has three sections - one in the middle, under the tapered T-junction and two others on each side, under each 1×2 monopole sub-array. The middle section of the ground plane beneath the tapered T-junction has been exponentially flared gradually to make a balanced line at the T-junction, whereas the other end of the T-junction, attached to the SMA connector, is an unbalanced line. Therefore, the design of the ground plane has been optimized to provide an unbalanced-to-balanced line transition

for impedance matching of the feeding network. To avoid backside radiation, a metal reflector is attached below the ground plane at a distance of h. The antenna and the metal reflector are attached mechanically by plastic screws as shown in Fig. 1c. Four holes have been made at the four corners of the antenna substrate and the metal reflector to insert the screws. The antenna is designed on a Taconic RF-35 substrate with a thickness of 1.52 mm, a relative permittivity of 3.5, and a loss tangent of 0.0018 at 1.9 GHz. An end-launcher SMA connector attached to the microstrip feed line has been taken into account during the design and optimization of the proposed antenna in HFSS. The optimized dimensions of the proposed antenna array are listed in Table. I

TABLE I
OPTIMUM DIMENSIONS OF THE PROPOSED MONOPOLE ANTENNA

Parameter	R_W	R_L	W	L	t
Value (mm)	114	99.5	94	79.5	3
Parameter	s	D_1	D_2	t_a	m
Value (mm)	20.6	21.5	30.8	11.64	18
Parameter	n	p	q	g	h
Value (mm)	10	14	28.22	2	10

B. Phase Inverter Design and E-field Alignment

The monopole array elements are symmetrical with respect to the x-axis as shown in Fig. 1a. Symmetrical array elements, which are fed by a single-ended signal, produce co-polarized components of radiated E-fields that are of opposite directions, cancelling each other vectorially [18]. To visualize this concept, radiated electric fields from the four elements of the array fed with a single-ended signal (without phase inverter), denoted as $\vec{E}_1$, $\vec{E}_2$, $\vec{E}_3$, and $\vec{E}_4$ in an arbitrary direction, are illustrated in Fig. 2a. Each electric field vector can be decomposed into two vectorial components representing the co-polarized components ($\vec{E}_c$) and cross-polarized components ($\vec{E}_x$) with the corresponding numeric subscript. As can be seen from Fig. 2a, the co-polarized components are directed in opposite direction and thus, cancelling one another. To align the co-polarized components of the radiated E-fields in the same direction, a 180 degree phase inverter consisting of electronic vias and inter-digitated slot is placed in one of the arms of the feeding T-junction, see Fig. 2b. By inserting the phase inverter, the orientation of the co-polarized components are aligned in the same direction, yielding a high gain. Fig. 3a shows the three dimensional view of the designed phase inverter. The signal and ground planes are swapped with the aid of vias, obtaining 180-degree difference in phase. The electronic vias are of hollow cylindrical type, having a diameter of $k = 0.3$ mm, and a height of $e = 1.52$ mm, complying with the standard of printed circuit board fabrication technology. The optimum dimensions of the phase inverter are as follows: $a = 0.2$ mm, $b = 2.5$ mm, $c = 1.25$ mm, and $d = 0.3$ mm. Fig. 3b provides the phase response diagram after inserting the phase inverter in the feeding network. The designed phase inverter perform very well because the simulated phase difference is 179.4° at 2.75 GHz and 186.9° at 4.7 GHz, as shown by point A and B respectively.

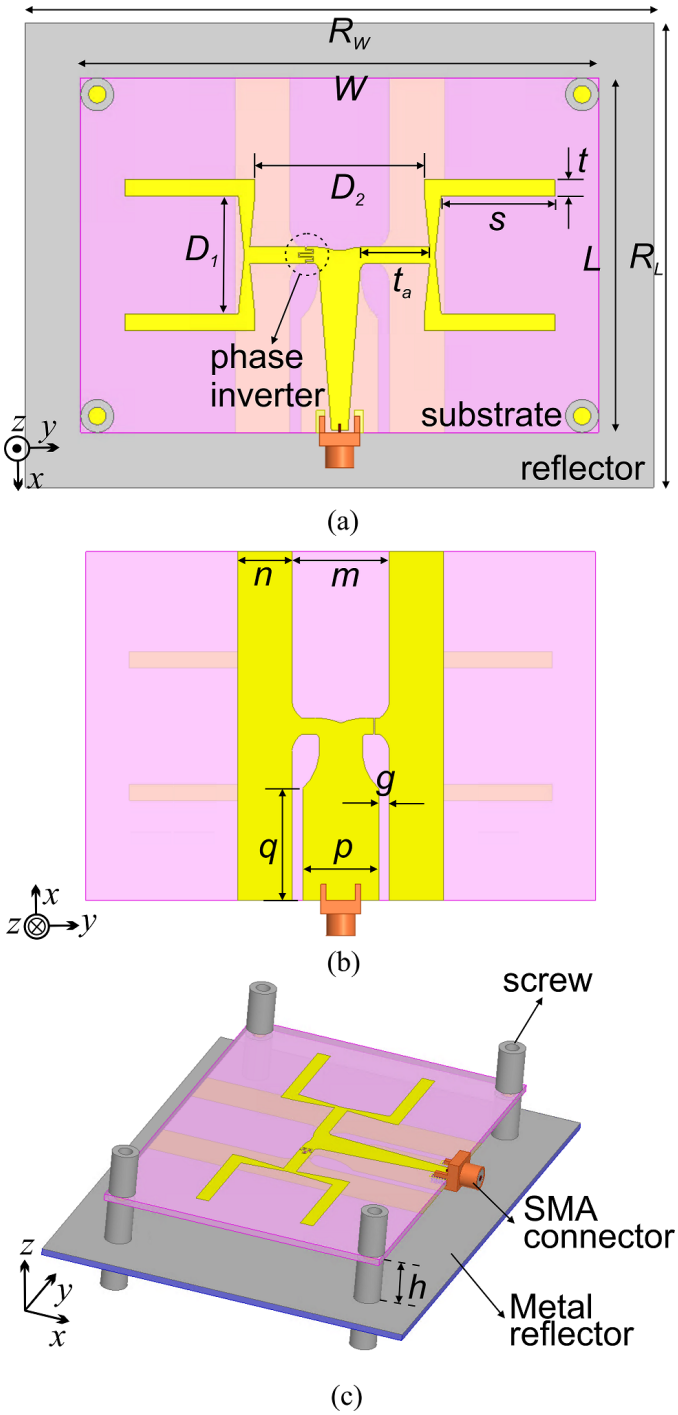

Fig. 1. Proposed antenna array (a) top view, (b) ground plane, (c) with the metal reflector attached to the antenna.

III. Results and Discussion

A. Simulated Results

The numerical simulations are performed in finite-element-method-based electromagnetic solver ANSYS HFSS. Fig. 4

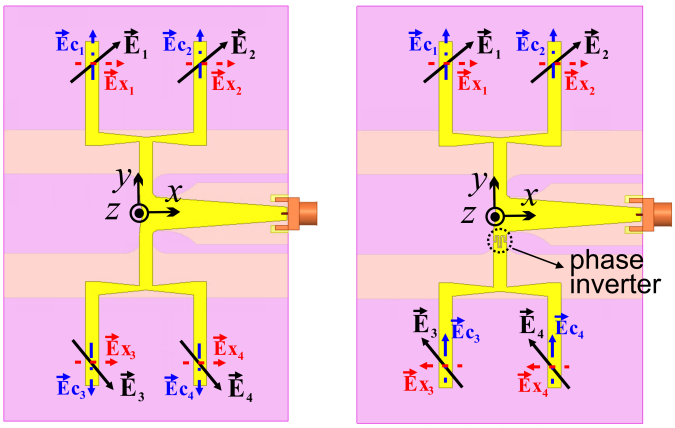

(a) (b)

Fig. 2. Visualization of the radiated electric fields in the proposed antenna array (a) without phase inverter, (b) with phase inverter.

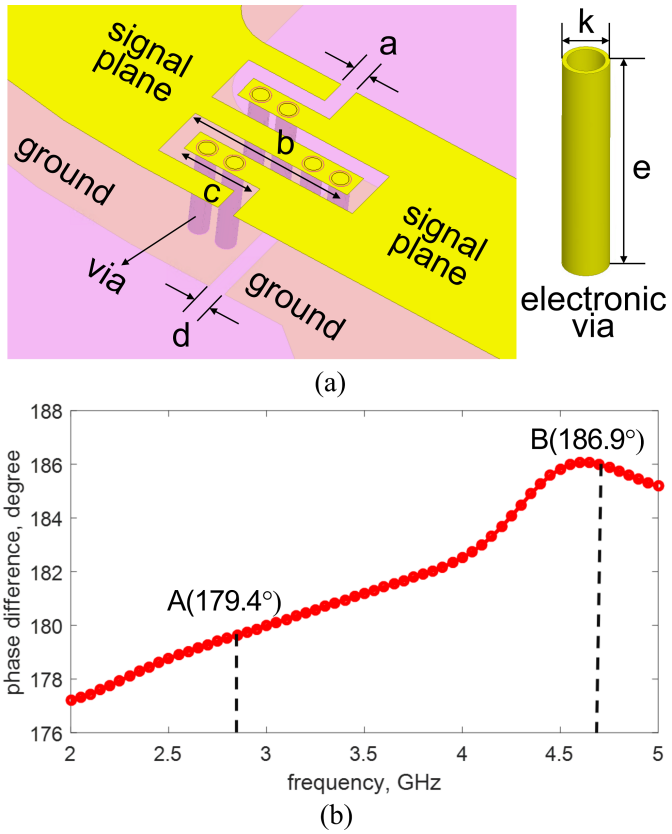

(a) (b)

Fig. 3. (a) Three dimensional view of the 180 degree phase inverter and (b) its phase response.

compares the reflection coefficient, $|S_{11}|$, of the proposed antenna array with and without the phase inverter. Although both curves in Fig. 4 follow a similar trend with clear dual resonances at about 2.75 GHz and 4.7 GHz, the impedance matching has been improved after inserting the phase inverter into the system. A slight shift in the reflection coefficient is observed after introducing the phase inverter, which could be anticipated as any practical microwave system introduces insertion loss and shifts the overall s-parameters of the system [19]. The operating impedance bandwidth of the proposed antenna array is 2.65–2.85 GHz and 4.66–4.76 GHz where $|S_{11}| \leq -10$ dB. The three dimensional radiation patterns of the proposed antenna array at 2.75 GHz and 4.7 GHz are shown in Fig. 5a and Fig. 5b, respectively. As seen from the radiation patterns, the maximum radiation patterns occur at the top of the antenna array, i.e., along z-axis, due to the metal reflector in the back of the antenna.

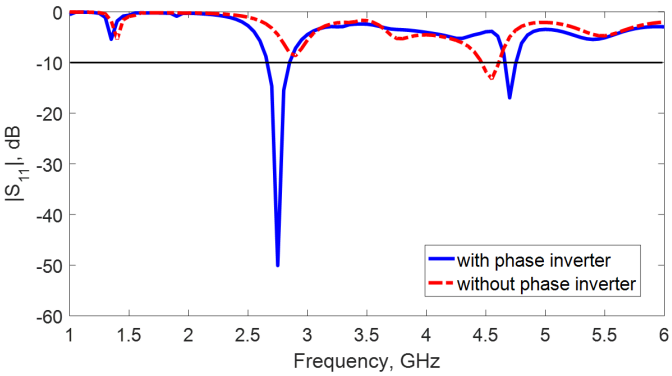

Fig. 4. Simulated reflection coefficient of the proposed antenna array.

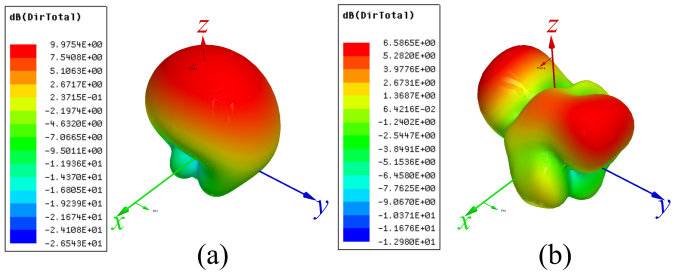

(a) (b)

Fig. 5. Radiation patterns of the proposed antenna array at (a) 2.75 GHz, and (b) 4.7 GHz.

Fig. 6 shows the simulated peak gain of the antenna array. For the purpose of comparison, three cases are examined- *(i)* the proposed antenna array, *(ii)* the array without the phase inverter but with the reflector, and *(iii)* the array without the reflector but with the phase inverter. Simulated results shows that the maximum value of the peak gain can be achieved when the antenna array is equipped with both the phase inverter and the reflector. As discussed in earlier sections, the phase inverter aligns the radiated fields in the same directions, increasing the peak gain of the antenna, whereas the backside reflector reflects all back-side radiated wave upward which also contributes in the increment of the peak gain. The simulated peak gain of the proposed antenna array is 10 dBi and 6.51 dBi at 2.75 GHz and 4.7 GHz, respectively. The magnitude of the surface current densities of the proposed antenna array at 2.75 GHz and 4.7 GHz are provided in Fig. 7.

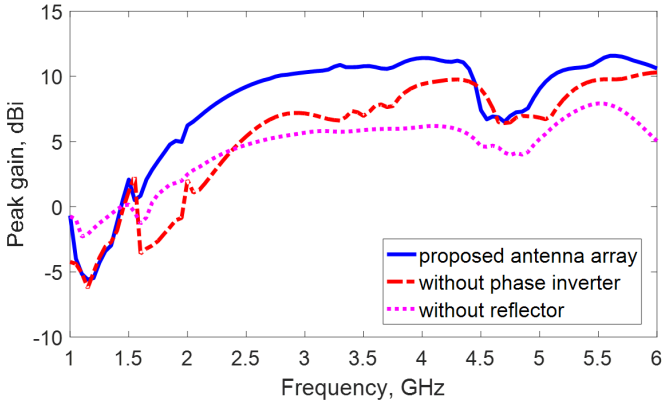

Fig. 6. Simulated peak gain of the proposed antenna array.

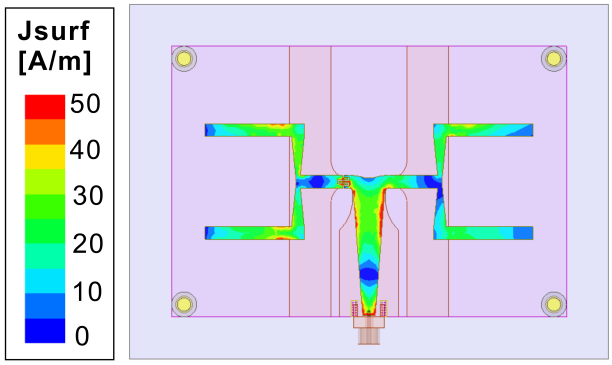

(a)

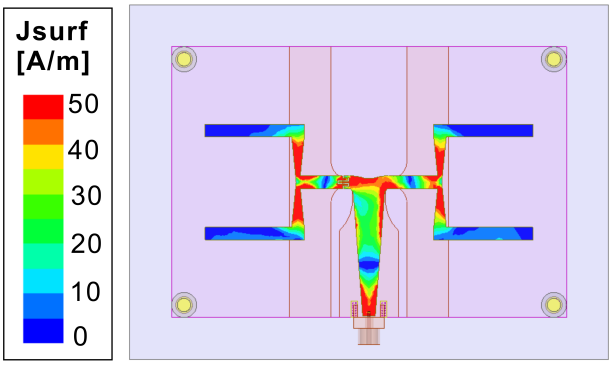

(b)

Fig. 7. Surface current density of the proposed antenna array at (a) 2.75 GHz, and (b) 4.7 GHz.

B. Effect of The Metal Reflector Separation

Since the proposed antenna array employs a back-side metal reflector placed beneath the substrate, the distance of h from reflector to the substrate plays an important role in the antenna optimization. By varying the values of $h = 5$, 10, and 15 mm, the effect of the distance h on the reflection coefficient is observed in Fig. 8. The parametric simulation results indicate that the reflection coefficient of the proposed antenna array show comparatively better impedance matching when the metal reflector is placed at a distance of $h = 10$ mm underneath the substrate. The reason underlying the phenomenon can be explained by considering the capacitive effect between the metal plate and the radiating array elements. Since the capacitance depends on the distance, the variation of h yields completely different capacitive effect and thereby, changing the overall reflection coefficient of the antenna array.

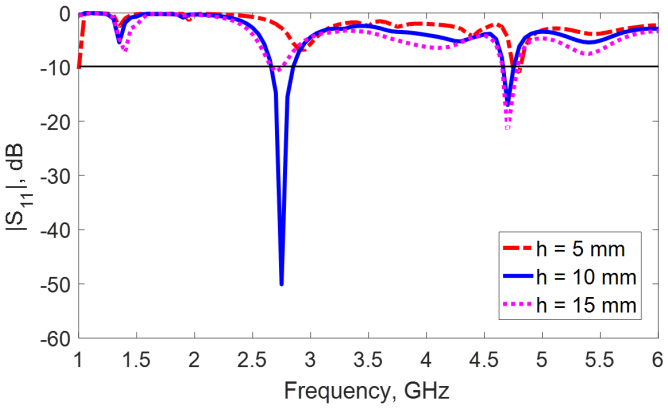

Fig. 8. Effect of the distance of metal reflector (h) on reflection coefficient of the proposed antenna array.

IV. Conclusion

A dual band monopole antenna array with a 180 degree phase inverter and a metal reflector is proposed and investigated. It operates at 2.75 GHz and 4.7 GHz. The on-board phase inverter, utilizing the application of the principle for vectorial addition of radiated fields is placed in one of the T-junction arms to yield maximum gain. The aim of the backside reflector is to keep the radiation patterns broadside. To achieve the best impedance matching, the metal reflector is placed at a distance of 10 mm from the substrate. The achieved peak gains are 10 dBi (at 2.75 GHz) and 6.51 dBi (at 4.7 GHz). The proposed antenna array is suitable for wireless communications.

Acknowledgment

This work has been supported by *Tensorbundle Lab*. The authors wish to thank fellow members of the Oxford Metamaterials Network (OxiMETA) for fruitful discussions.

References

[1] M.N. Hasan, S. Chu, and S. Bashir, "A DGS monopole antenna loaded with U-shape stub for UWB MIMO applications," *Microw. Opt. Technol. Lett.*, May, 2019. DOI: 10.1002/mop.31877.

[2] M.N. Hasan, and M. Seo, "Compact omnidirectional 28 GHz 2×2 MIMO antenna array for 5G communications," *23rd International Symposium on Antennas and Propagation (ISAP)*, Busan, South Korea, Oct. 2018.

[3] M.N. Hasan, and M. Seo, "A Planar 3.4–9 GHz UWB Monopole Antenna," *23rd International Symposium on Antennas and Propagation (ISAP)*, Busan, South Korea, Oct. 2018.

[4] S. Chu, M.N. Hasan, J. Yan, and C.C. Chu, "A planar super wideband annular ring monopole antenna with time domain characterization," *30th Asia-Pacific Microwave Conference (APMC)*, Kyoto, Japan, Nov. 2018.

[5] M.N. Hasan, P. Singh, and M.D. Nadeem, "Omnidirectional UWB antenna loaded with rectangular loop for band notch characteristics," *6th International Conference on Signal Processing and Integrated Networks (SPIN)*, pp. 425–429, Noida, India, Mar. 2019.

[6] S. Chu, M.N. Hasan, J. Yan, and C.C. Chu, "Tri-band 2×2 5G MIMO antenna array," *30th Asia-Pacific Microwave Conference (APMC)*, Kyoto, Japan, Nov. 2018.

[7] H.Y. Chien, C.Y.D. Sim, and C.H. Lee, "Dual-band meander monopole antenna for WLAN operation in laptop computer," *IEEE Antennas Wireless Propag. Lett.*, vol. 12, pp. 694–697, May 2013.

[8] J.W. Park, M.J. Jeong, N. Hussain, H.U. Bong, and N. Kim, "Design of a dual-band planar monopole antenna for WLAN applications," *International Symposium on Antennas and Propagation (ISAP)*, Oct. 2018, Busan, South Korea.

[9] W.K. Toh, and Z.N. Chen, "Tunable dual-band planar antenna," *Elec. Lett.*, vol. 44, no. 1, pp. 8–9, Jan. 2008.

[10] X.W. Dai, T. Zhou, and G.F. Cui, "Dual-band microstrip circular patch antenna with monopolar radiation pattern," *IEEE Antennas Wireless Propag. Lett.*, vol. 15, pp. 1004–1007, Oct. 2015.

[11] K. He, S.X. Gong, and F. Gao, "A wideband dual-band magneto-electric dipole antenna with improved feeding structure," *IEEE Antennas Wireless Propag. Lett.*, vol. 13, pp. 1729–1732, Aug. 2014.

[12] M.N. Hasan, S.W. Shah, M.I. Babar, and Z. Sabir, "Design and simulation based studies of a dual band u-slot patch antenna for WLAN application," *14th International Conference on Advanced Communication Technology (ICACT)*, PyeongChang, South Korea, Feb. 2012.

[13] K. He, S.X. Gong, and F. Gao, "Gain enhancement of a broadband symmetrical dual-loop antenna using shorting pins," *IEEE Antennas Wireless Propag. Lett.*, vol. 17, no. 8, pp. 1369–1372, Aug. 2018.

[14] P. Prakash, M.P. Abegaonkar, A. Basu, and S.K. Koul, "Gain enhancement of a CPW-fed monopole antenna using polarization-insensitive AMC structure," *IEEE Antennas Wireless Propag. Lett.*, vol. 12, pp. 1315–1318, Oct. 2013.

[15] H. Wang, S.F. Liu, L. Chen, W.T. Li, and X.W. Shi, "Gain enhancement for broadband vertical planar printed antenna with H-shaped resonator structures," *IEEE Trans. Antennas Propag.*, vol. 62, no. 8, pp. 4411–4415, May 2014.

[16] M.N. Hasan, and M. Seo, "High-gain 2×2 UWB antenna array with integrated phase inverter," *Elec. Lett.*, vol. 54, no. 10, pp. 612–614, May 2018.

[17] M.N. Hasan, R.B.V.B. Simorangkir, K.P. Esselle, and S. Shad, "Differentially fed CDRA array with phase inverter for high gain and reduced cross polarization," *IEEE Int. Symp. on Antennas and Propag. USNC/URSI National Radio Science Meeting*, Jul. 2019, Atlanta, USA.

[18] G. Adamuik, M. Pauli, and T. Zwick, "Principle for the realization of dual-orthogonal linearly polarized antennas for UWB technique," *Int. J. Antennas Propag.*, vol. 11, 2011.

[19] D.M. Pozar, "Microwave Engineering," *4th Ed., John Wiley and Sons, Inc.*, Nov. 2011.